metals

Article

Beneficiation of Low-Grade Dilband Iron Ore by Reduction Roasting

Ali Dad Chandio [1,*], Iftikhar Ahmed Channa [1], Asif Ahmed Shaikh [1], Shabbir Madad [1], Syed Bilal Hasan Rizvi [1], Aqeel Ahmed Shah [1], Jaweria Ashfaq [1], Muhammad Ali Shar [2] and Abdulaziz Alhazaa [3]

1 Department of Metallurgical Engineering, NED University of Engineering and Technology, Karachi 75270, Pakistan
2 Department of Mechanical & Energy Systems Engineering, Faculty of Engineering and Informatics, University of Bradford, Bradford BD7 1DP, UK
3 Department of Physics and Astronomy, College of Science, King Saud University, Riyadh 11451, Saudi Arabia
* Correspondence: alidad@neduet.edu.pk

Abstract: This research is aimed at the up-gradation of indigenous Pakistani iron ore, i.e., Dilband iron ore (hematite), by utilizing common metallurgical processes. First, the magnetic properties of the ore were determined. Initially, the iron ore samples contained 34 wt. % Fe in addition to other gangue materials. Therefore, the ore was subjected to a high-temperature reduction roasting process between 800 °C and 1000 °C. Additionally, the magnetic separation process was also employed. The influence of different roasting parameters, such as the reduction time, coal-to-ore ratio, and temperature, was examined. This was followed by characterization techniques using XRD (X-ray diffraction analysis), the Rietveld method, wet chemistry analysis, and a VSM (Vibrating Sample Magnetometer). The results suggest an excellent reduction at 900 °C for a coal/ore ratio of 20 wt. %, which was achieved within 2 h of the process. The Fe concentration increased tremendously from 34 to 56 wt. %, and in conjunction, magnetic properties were also induced (1.5 emu). The recovery was found to be substantial for the ore when the Fe content was 75 wt. %. Additionally, the economic feasibility of the processed ore was also studied, followed by an extensive analysis of the roasting and magnetic separation processes.

Keywords: hematite; magnetite; roasting; XRD; Rietveld analysis; VSM

Citation: Chandio, A.D.; Channa, I.A.; Shaikh, A.A.; Madad, S.; Rizvi, S.B.H.; Shah, A.A.; Ashfaq, J.; Ali Shar, M.; Alhazaa, A. Beneficiation of Low-Grade Dilband Iron Ore by Reduction Roasting. *Metals* **2023**, *13*, 296. https://doi.org/10.3390/met13020296

Academic Editor: Alexander Babich

Received: 1 November 2022
Revised: 20 January 2023
Accepted: 25 January 2023
Published: 1 February 2023

1. Introduction

Dilband iron ore is a stratiform iron ore deposit discovered in 1997 by the Geographical Survey of Pakistan in the Kalat division of Baluchistan, Pakistan. It was initially estimated that this deposit could yield 200 million tons of ore containing about 34–45% iron content along with 18–20% silicate. Dilband ore can be considered one of the most challenging iron ores [1,2].

The iron ore primarily consists of ooids, mostly composed of hematite pellets embedded in a calcite matrix. Irregular hematite fragments were discovered that were naturally enriched with quartz, kaolinite, and clinochlore contents [3]. The second widely found stone geometry is that of peloids composed of pellets of hematite fragments embedded in a calcite matrix. Peloids also contain quartz content. Another iron ore type is biosparite, which is mostly composed of hematite bioclasts. Therefore, most of the minerals found in Dilband iron ore are hematite, quartz, calcite, kaolinite, clinochlore, and fluorapatite [4].

Dilband iron ore is inappropriate for blast furnace operation due to its excessive silica and alumina contents [5], which generate operational problems in smelting, such as creating more slag, requiring more heat energy, and disturbing the melt chemistry. Gangue minerals, specifically silica, cannot be easily separated from the concentrate using conventional beneficiation techniques. Additionally, phosphorous is disseminated in the matrix, leading to other operational issues [6]. To liberate hematite from the gangue minerals, its size must be reduced to 5 µm [7]. Flocculation was proposed as a suitable method for the beneficiation of ore, but it also proved to be inadequate [8].

Considering the challenges in the beneficiation of Dilband iron ore, an alternative route needs to be utilized. Magnetic roasting is a possible alternative route to counter these challenges, and it has proved to produce high yields from low-grade iron ores [9]. Magnetic roasting consists of reduction roasting followed by magnetic separation. Reduction roasting transforms hematite into magnetite [10], which is magnetic and easily separated using a magnetic influence [11]. The process of the reduction of hematite to magnetite occurs as a consequence of chemical reactions, and these reactions are given in Equations (1)–(3) [1]:

$$C + O_2 \rightarrow CO_2 \tag{1}$$

$$CO_2 + C \rightarrow 2CO \tag{2}$$

$$3Fe_2O_3 + CO \rightarrow 2Fe_3O_4 + CO_2 \tag{3}$$

Dilband iron ore falls into the category of complex low-grade iron ore, where silicate and phosphorous are present as impurities [12]. The direct reduction of this type of ore was found to be much more practicable, and intermetallic phase growth was also observed [13]. Research has proved that the magnetic separation after roasting is influential on low-grade iron ore, which was unaffected by other beneficiation techniques, such as froth flotation and direct magnetic separation [14].

Reduction roasting has great potential to be utilized to process low-quality iron ore, but no such practices have been carried out on Dilband iron ore [15]. Therefore, in order to realize the true potential of this locally available ore deposit, the beneficiation of Dilband ore is carried out. In this study, an investigation was performed via maintaining a reducing environment. This step is performed to convert hematite into magnetite so that the magnetic characteristics can be utilized at later stages [16,17]. Magnetic and non-magnetic contents were separated as tailings and concentrated using a magnetic drum separator. Further, characterization techniques were employed to study the changes in phases during the process [18,19]. Furthermore, the feasibility of the high-temperature reduction roasting process was also evaluated. This may help in understanding the cost–benefit analysis of the process if Dilband ore is put forward for commercial utilization for its use as a feed for iron and steel production.

The elemental analysis showed that most of the elements are distributed in the size range from 38 µm to 600 µm. It was further noted that the iron content tends to decrease and the calcite content increases as the ore size is reduced [4]. Grinding ore is an energy- and cost-intensive task. The cost relates not only to the operation but also to the wear and breakdown of mills and machinery due to the grinding process. The grindability of Dilband ore was calculated by measuring the surface area per unit energy with various grinding cycles [20]. It was estimated that the energy per unit increases as the number of grinding cycles increases. Then, a slight decrease was recorded, and 2.2 kilowatts per hour of energy was required to reduce the size of Dilband iron ore from 3800 µm to 82 µm at 80% passing [21].

The iron ore obtained from the mining area having an iron content of more than 56% is used in the industry, whereas iron ore with a low quantity of iron in its ore form is rejected. In the past few years, the study of low-quality mineral ore has been attempted by a few researchers to replace high-quality mineral ore. In connection to that, this study was carried out to obtain an ore with an Fe content of around 56%, with a recovery rate of 75%, from iron ore having 33 wt. % iron content. One of the objectives of this study is to realize the true importance of locally available iron ore deposits. The results of this study may serve as supporting evidence to boost indigenous mining and other related industries in Pakistan, as encouraging results were obtained in this study [22].

2. Materials and Methods

2.1. Materials

Dilband iron ore, which is an abundantly available resource in Pakistan, was received from "Bolan Mining Enterprises" and used in its as-received condition, and coal powder with 98% purity was purchased from "Merck Sigma-Aldrich" and was utilized for the reduction of iron ore.

2.2. Methods

As shown in Figure 1, the reduction of low-quality hematite into magnetic iron ore can be completed in three steps: it starts with ball milling the raw ore, and then the ore is reduced in the presence of coal, followed by processing using a drum wet weak magnetic separator. The final product contains a magnetic compound of iron oxide, which can be easily extracted from the tailings/impurities.

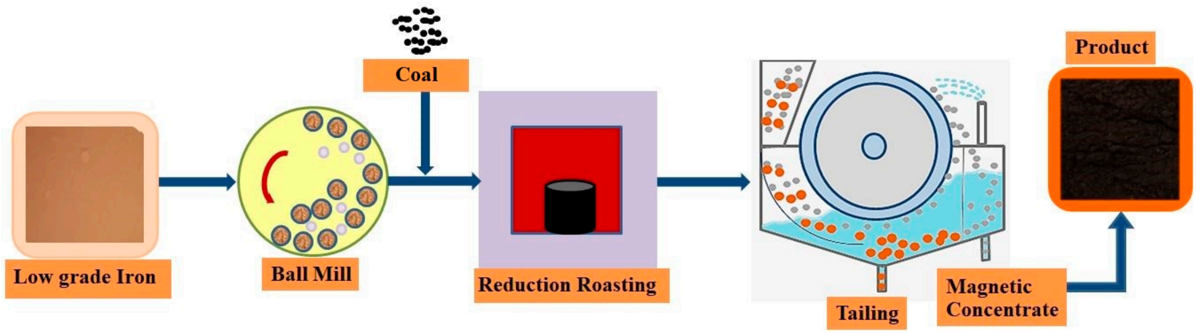

Figure 1. Step-by-step process of reduction roasting process.

Figure 2 illustrates the interaction of iron oxide with CO and CO_2 in different proportions, and reaction 1 in the figure indicates the low concentrations of CO and CO_2 required for the reduction reaction [12]. Higher concentrations will lead to an inefficient, incomplete reduction, and as this reaction is irreversible, an incomplete reduction cannot be reverted [23].

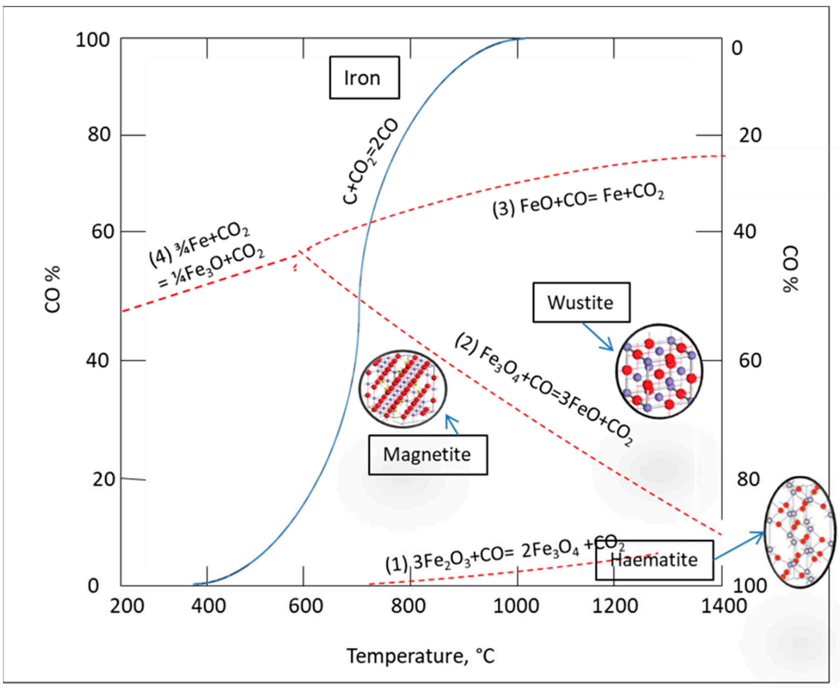

Figure 2. Roasting and reduction processes. Adapted from Ref. [24].

Hematite reduction can be influenced by impurities present in the ore. Therefore, research has been carried out to perform magnetic separation after roasting low-grade iron ore [25,26].

2.2.1. Crushing

Dilband iron ore was received in big lumps. To reduce it to a smaller size, a crusher was used. For this purpose, the jaw crusher from "Yantai Jinyuan Mining Machinery Co., Ltd." was used to reduce the big lumps into smaller stones. Later on, a ball-milling machine was used to reduce the crushed particles into small-sized powders. The "XMQ 350x160 Cone Ball Mill from Yantai Jinyuan Mining Machinery Co., Ltd." was utilized for this purpose. The powder was reduced to about <100 μm for reduction roasting. According to previous research [27,28], Dilband ore requires excessive energy to be reduced, and the ball mill's efficiency was increased by using a more significant number of steel balls and a low feed. The ball mill used has a 4000-g total feed capacity; in support of the available conditions, the efficiency of the ball mill was increased by adding 1500~2000 g of the ore for 180 min each cycle.

2.2.2. High-Temperature Reduction Roasting

The roasting of iron ore is an important aspect to be processed in the calculation environment. For this purpose, a lab-scale furnace from "PRO THERM Laboratory Furnace PLF 120/10" (Pro Therm furnanes, Ankara, TURKEY) [29] was used to reduce the hematite content into magnetite. By roasting materials in a reducing environment at temperatures between 800 and 1000 °C, reduction roasting can transform non- or weakly magnetic minerals into magnetic minerals. The transition is more likely to be imperfect at lower temperatures (600–800 °C), while at higher temperatures, it is crucial to avoid over-reduction to prevent particle fusion or the development of paramagnetic wüstite.

2.2.3. Magnetic Separation

To distinguish the magnetic content from gangue materials, "The Drum Wet Weak Magnetic Separator of Yantai Jinyuan Mining Machinery Co., Ltd." was utilized, having a minimum feed of 500 g and DC input with a limit value of up to 5 amperes, along with a pressure regulator for the water supply [30].

2.3. Testing and Characterization

The effects of temperature and coal percentages were tested, and the results were observed. The processing steps were followed as per the work published by Dash et al. (2019) [31]. Coal percentages from 8 to 20 were considered, and two different temperatures were selected for reduction roasting. The treated samples were then water-quenched after the process to prevent excess transformation in the treated samples.

2.3.1. Sieving/Laser Particle Analysis

Sieve analysis was used to distinguish between powders of different sizes. For this purpose, "The Endecotts Octagon Digital Vibrating Sieve Shaker" was used, and particles below a 56 μm sieve were collected separately. Powder particles larger than the required size were sent for crushing again. The size selection of iron ore was also confirmed by using the Laser Particle Analysis technique using the "Bettersize BT-9300H Laser Particle Analyzer" instrument (Bettersize, Dandong, China).

2.3.2. Chemical analysis

To quantitatively analyze the iron (Fe) content of the ore, the chemical method was utilized. The chemical analysis of the concentrates was conducted using Ammonium Fluoride (NH_4F), Hydrochloric Acid (HCl), Per-chloric acid ($HClO_4$), Nitric acid (HNO_3), Phosphoric acid (H_3PO_4), and Mercuric chloride ($HgCl_2$), as shown in Figure 3.

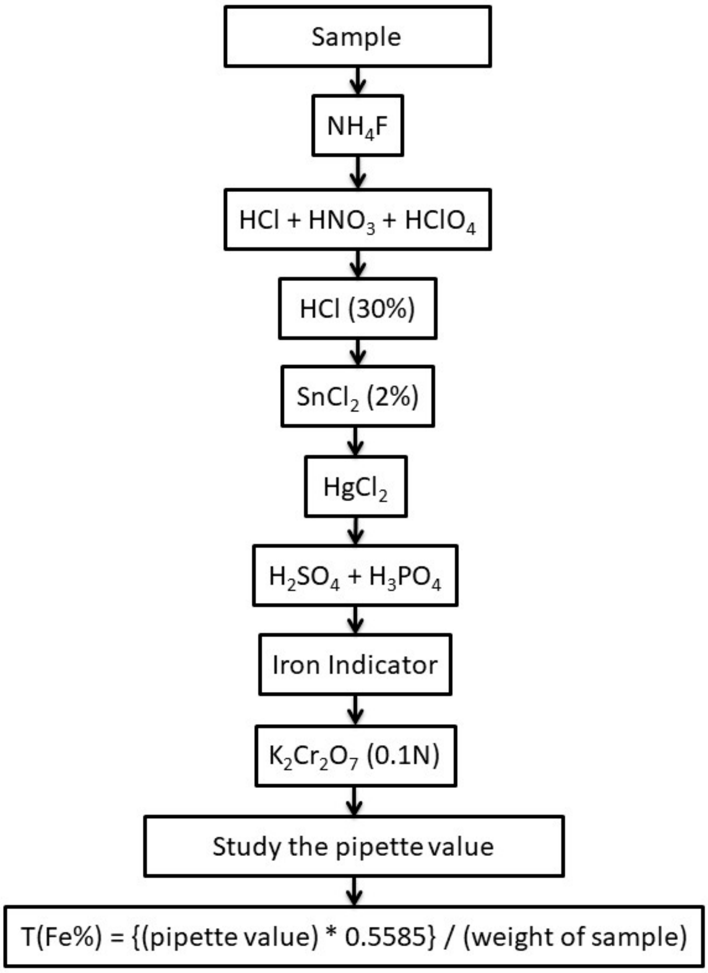

Figure 3. Flowchart for chemical analysis of Fe content.

2.3.3. XRD

X-ray diffraction analysis was used for structural characterization by using the XRD technique (utilizing PANalytical X'pert Pro, (Malvern, UK). In addition, to analyze the volume fraction or quantity of each phase, the Rietveld refinement technique was utilized using Profex software (version 4.2). The refinement focused on elements/compounds that were present in significant quantities. During refinement, peaks from the crystallite and micro-strain were analyzed where necessary. Moreover, texture refinement at different anisotropic levels was determined using the GEWICHT scale factor of refinement. It defines a series of symmetrical spherical harmonics at different levels, ranging from Sharp 0 to Sharp 8. The goodness of fit based on the weighted profile residual and expected profile residual (R/E) was kept under the limit of $x^2 < 1.5$. Moreover, the standard deviation of the whole refinement remained within the range of ~2% [32,33].

2.3.4. VSM

Processed samples were examined to understand their magnetic behavior using a VSM (MicroSense FCM-10, MA, USA) having a maximum field of up to 3.0 T and an accuracy of ±1%. The maximum limit for the sample was 10 g for a dynamic magnetization range between 1000 emu and 100 emu [34]. In these conditions, several randomly selected ore samples were analyzed to obtain representative values of the magnetic field.

2.4. Recovery and Grade Calculations

Mineral recovery is the ratio of the valuable minerals present in the concentrate to the amount of feed input. This was determined by using the following:

$$\text{Recovery} = \frac{c\,(f-t)}{f\,(c-t)}100\% \tag{4}$$

Here, f is the feed metal assay, c is the concentrate assay, and t is the tailing assay.

Another vital aspect is separation efficiency, which determines the percentage of gangue minerals present in the feed and the concentrate [35]. The following equation was used to determine it.

$$\text{Separation efficiency} = \frac{Mc}{Mf}\cdot\frac{(c-f)}{(m-f)}100\% \tag{5}$$

Here, m represents the metal grade, and M_c and M_f represent the mass of the feed and the mass of the concentrate, respectively [36].

3. Results and Discussion

3.1. Reduction Roasting

The reduction of hematite to magnetite is influenced by three significant factors, i.e., time, temperature, and the coal-to-ore ratio. Therefore, to determine the appropriate combination of factors for the optimal output, some of these factors were studied, and Figures 4 and 5 present the results obtained. It is evident from Figure 4 that the longer the time, the higher the reduction ratio, which indicates the better conversion of the ore into magnetite. This result is also in line with the literature [31], wherein a high temperature (above 700 °C) is recommended for low-grade iron ores.

Coal Ratios

In Figure 4, the graph illustrates the effects of altering the coal-to-ore ratio and time on the reduction while maintaining a constant temperature of 800 °C. While maintaining these parameters, about 33 wt. % of the hematite content present in the raw ore was successfully reduced to magnetite. However, this reduction rate is still insufficient to prove the importance of Dilband ore. Figure 5 shows the outcomes of increasing the time and coal ratio in order to raise the reduction rate and achieve the best result.

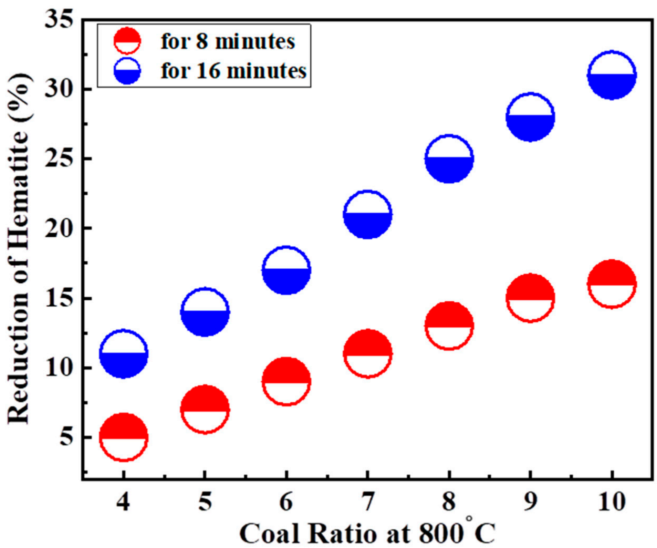

Figure 4. Effect of coal ratio at 800 °C for the reduction of hematite.

The coal-to-ore ratio was increased from 10 to 20%. In addition to this, the temperature and time were also increased and maintained at 900 °C for a maximum of 120 min. A higher temperature and longer roasting time resulted in an excellent reduction rate of hematite, i.e., about 100 wt. %. This is almost the same trend as in Figure 4 but with greatly improved output because the longer time and higher temperature enhanced the reduction percentage. Similarly, when a low coal-to-ore ratio was used for roasting, the temperature and time became less influential. Increasing the coal-to-ore ratio enhanced the influence of time and temperature, as depicted in Figures 4 and 5, and the most promising result of reduction was achieved by roasting at 900 °C for 2 h with a coal-to-ore ratio of 20 wt. %, which led to the maximum hematite reduction.

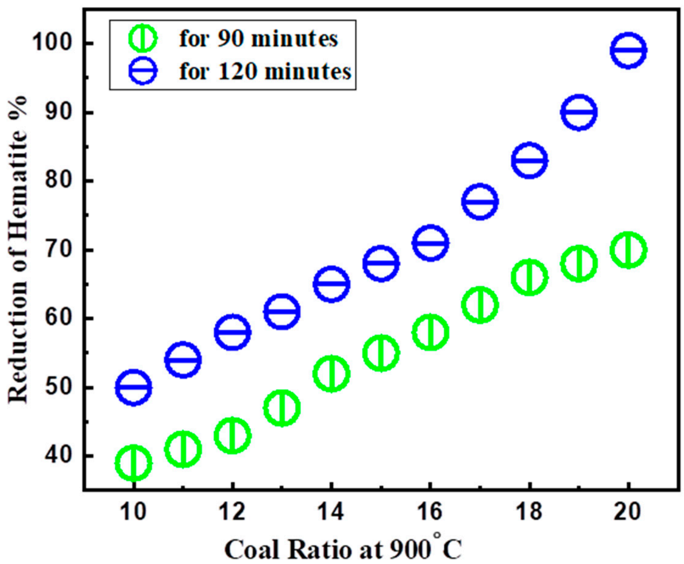

Figure 5. Effect of coal ratio at 900 °C for reduction of hematite.

Since higher temperatures and coal contents lead to the excessive reduction of hematite, forming weak magnetic ferrous oxide, it reduces the separation efficiency, subsequently decreasing the recovery of iron from gangue minerals. Hence, the temperatures selected were 800 °C to 900 °C. This temperature range is not commonly used for ore roasting reduction; however, particularly for Dilband ore, encouraging results were obtained while keeping the coal-to-ore ratio at 20 wt. % [18].

3.2. XRD

X-ray diffraction was used for the identification of phases in the raw ore and treated samples. Three samples of different compositions were studied in the analysis, as they were influenced by the magnetic field generated by a bar magnet. A color change during reduction roasting was also observed, from reddish hematite to a dark gray reduction product, as shown in Figure 6.

In Figure 7, the change in color is demonstrated through XRD results. The raw ore consisted of iron in two major forms: hematite and alpha iron. The raw iron was then separated into three different samples with variable compositions: sample 1 with 8 % coal at 800 °C for 16 min, sample 2 with a 20% coal ratio at 900 °C for 90 min, and sample 3 with a 20 % coal ratio at 900 °C for 120 min. All three samples are presented in Figures 7–9. Alpha iron was detected as the iron liberated from the gangue particles during the milling operation. The lattice parameters of hematite with space group 167 were identified as a = 0.503 nm and c = 1.37 nm, which are identical to the lattice parameters mentioned in the powder diffraction database. The peaks related to hematite (2θ = 24.0°, 35.6°; Reference codes: 01-073-0603 and 00-039-1346) started to diminish as the coal ratio, time, and temperature increased. Moreover, the peaks identifying magnetite (2θ = 33.22°, 35.662°, 57.42°; Reference codes: 00-003-0863 and 01-077-1545) became more prominent. Milling caused the quartz phase to include, which is known as an inclusion.

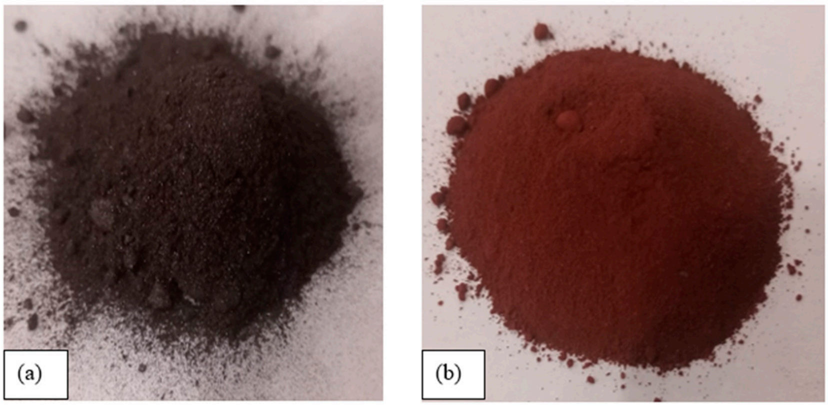

Figure 6. Difference in appearance of (**a**) processed and (**b**) raw/unprocessed ore.

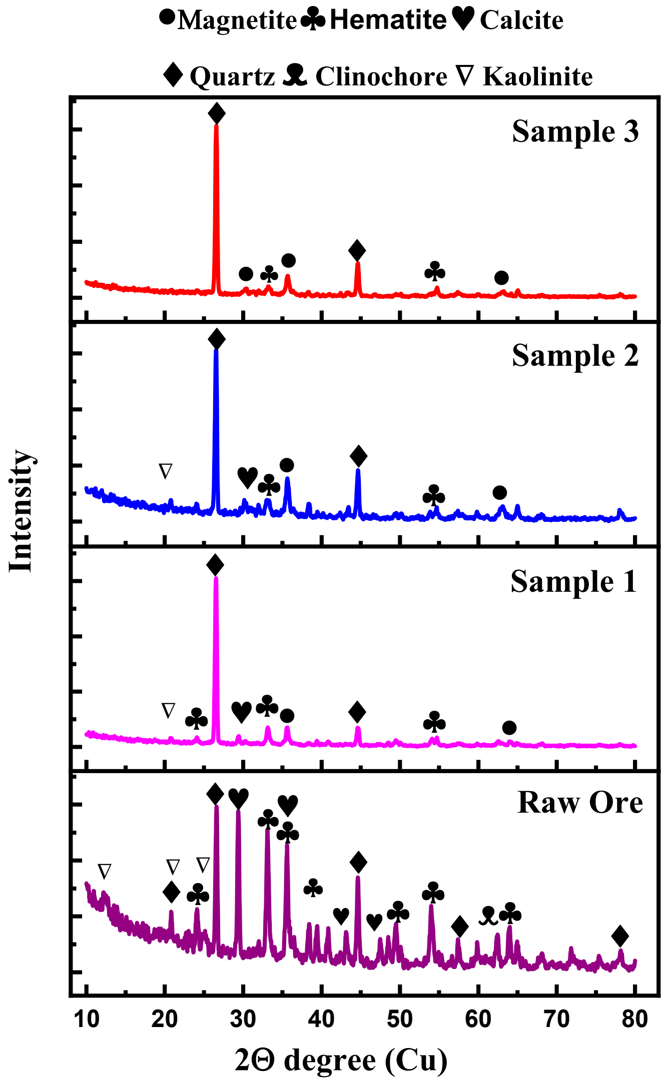

Figure 7. XRD results of raw and roasted ore at different temperatures.

Phase identification was carried out on the processed samples; they were divided into separate entities having different concentrates and tailings. Figure 8 shows the analysis of the concentrate obtained after the reduction process with the variable contents discussed earlier.

Figure 8 represents the data obtained from the Rietveld analysis of the samples, taking the ore's main constituents under consideration. The data show the trends of the reduction of hematite, which was the main objective of reduction roasting.

This confirmed the presence of magnetite with the maximum quantity in the drum wet weak magnetic separator feed. Based on the results, sample 3 was selected for further processing and was divided into three parts, i.e., samples A, B, and C.

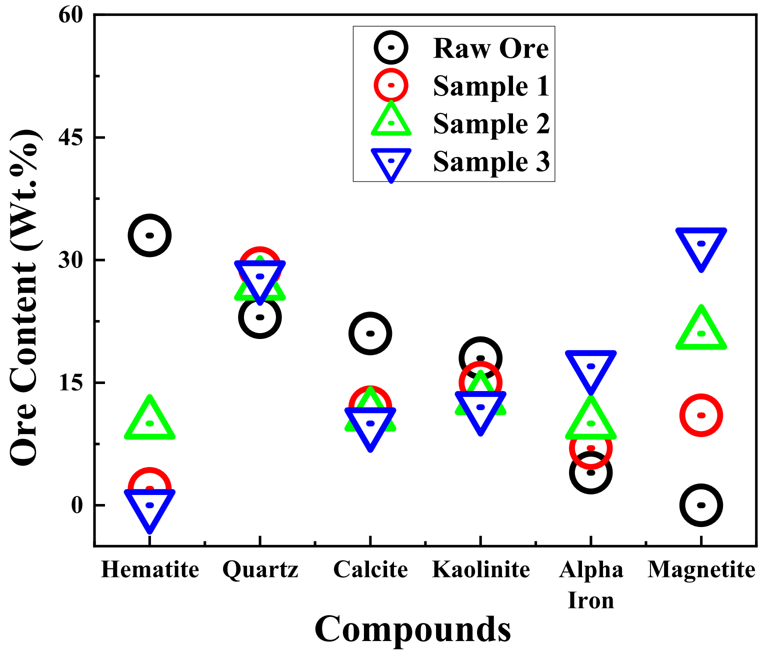

Figure 8. Rietveld analyses of 3 different samples after reduction reaction.

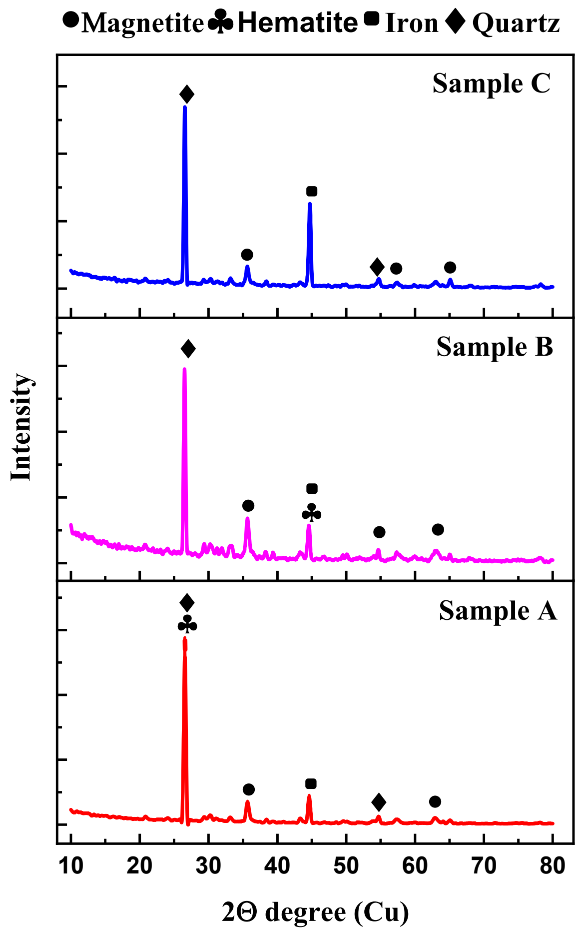

Figure 9. XRD results of concentrate from the drum wet weak magnetic separator.

XRD results were obtained after samples A, B, and C were subjected to the drum wet weak magnetic separator at three different current frequencies, i.e., 3 amperes, 4 amperes, and 5 amperes, respectively, as shown in Figure 10. Magnetite was clearly identified in all three samples. Moreover, free alpha iron and quartz were also present.

Rietveld refinement showed the optimal value of iron content at 57%, silicon at 7%, oxygen at 16%, and coal at 20% in the magnetic concentrate, as shown in Figure 10. The wt.% of iron content was further confirmed by the chemical analysis, as shown in Table 1.

Figure 10 characterizes the final product that contains the liberated iron at 56% and other contents at their optimal values. The final product is proposed to be sample C, which was processed at 900 °C for 120 min with 20% coal in a reducing environment. After the reduction, the product was processed with the drum wet weak magnetic separator with 5 amperes of current, which resulted in the optimal conditions for profitable/commercial use.

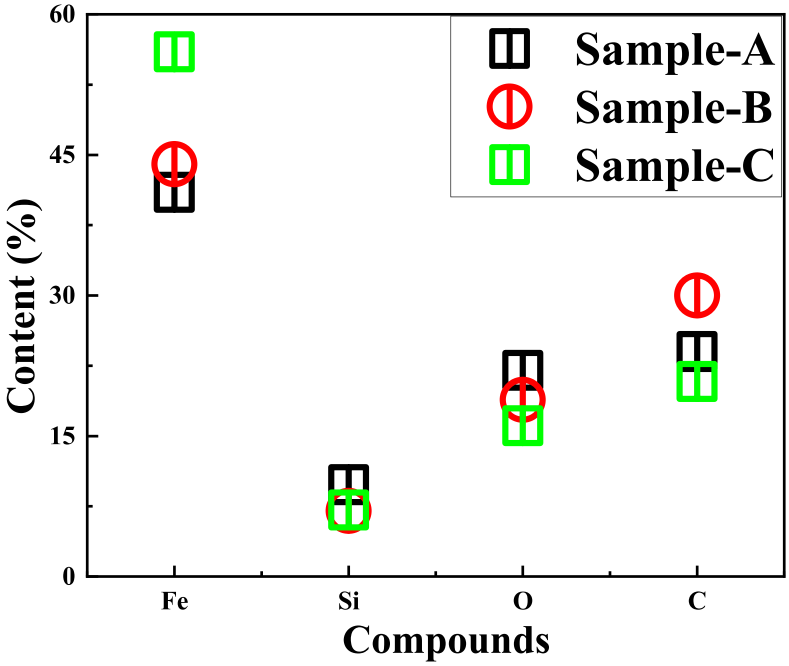

Figure 10. Concentrate from the drum wet weak magnetic separator. Concentrates A, B, and C were obtained at 3 amperes, 4 amperes, and 5 amperes, respectively.

Table 1. Chemical analysis of concentrates.

Samples	Fe Content (Wt.%)	Standard Deviation
Sample A	**39.20**	**±1.0**
Sample B	**44.00**	**±1.0**
Sample C	**55.12**	**±1.0**

3.3. VSM

The magnetic properties of the reduced iron ore were examined to establish the quantity of magnetite formed. It also confirmed that the effect of impurities remaining after the reduction on the magnetic behavior was minimal. Upon examining the plot, it was noticed that all three concentrates contained sufficient magnetic properties, and the concentrate containing the highest percentage of iron showed the highest magnetization.

In Figure 11, it can be observed that the saturation of samples in the field of 23 KOe was successfully reached. For sample C, the maximum magnetization reached 1.51 emu, while in the case of samples A and B, a maximum magnetization of 0.76 emus and 1.15 emus was recorded.

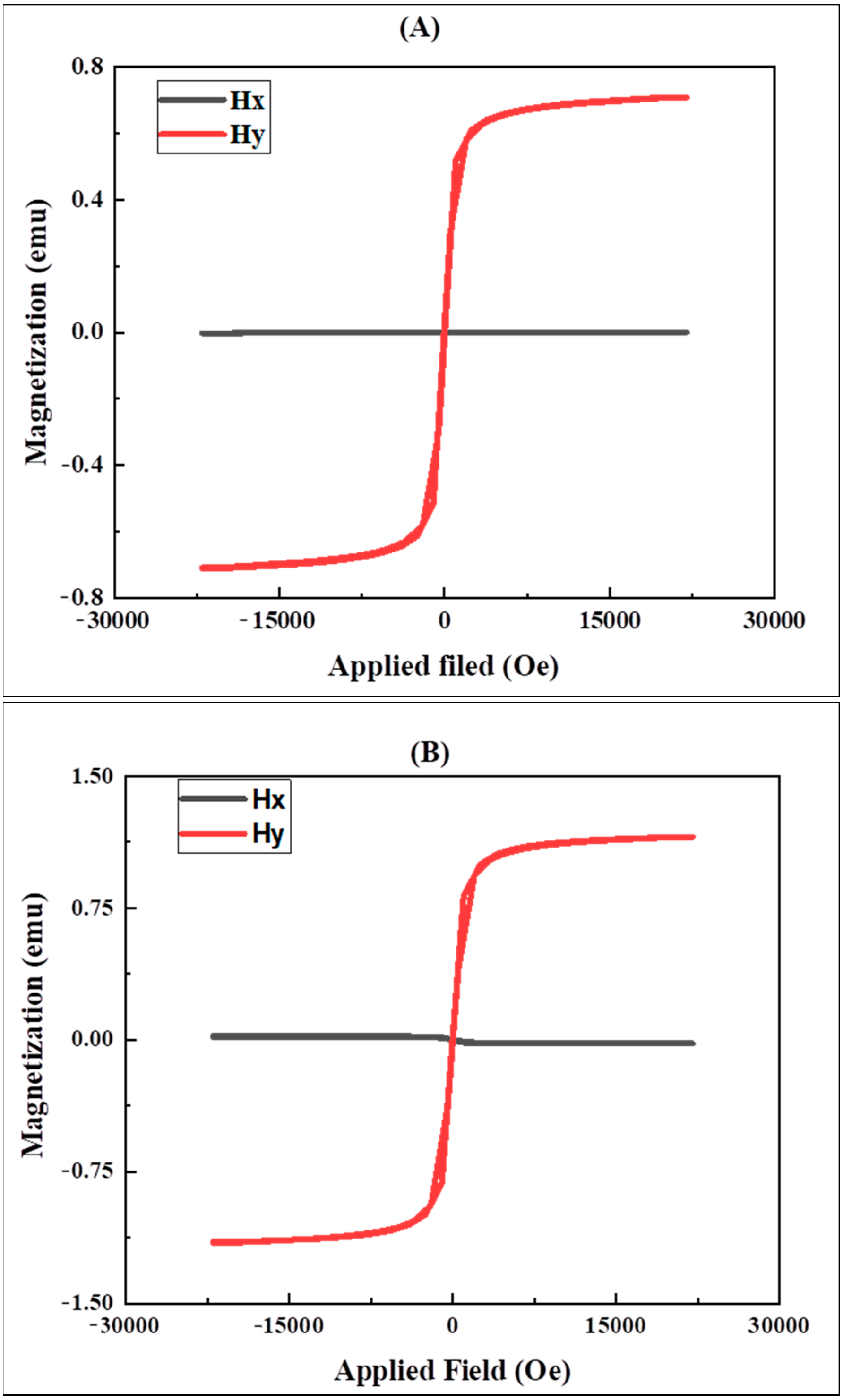

Figure 11. *Cont.*

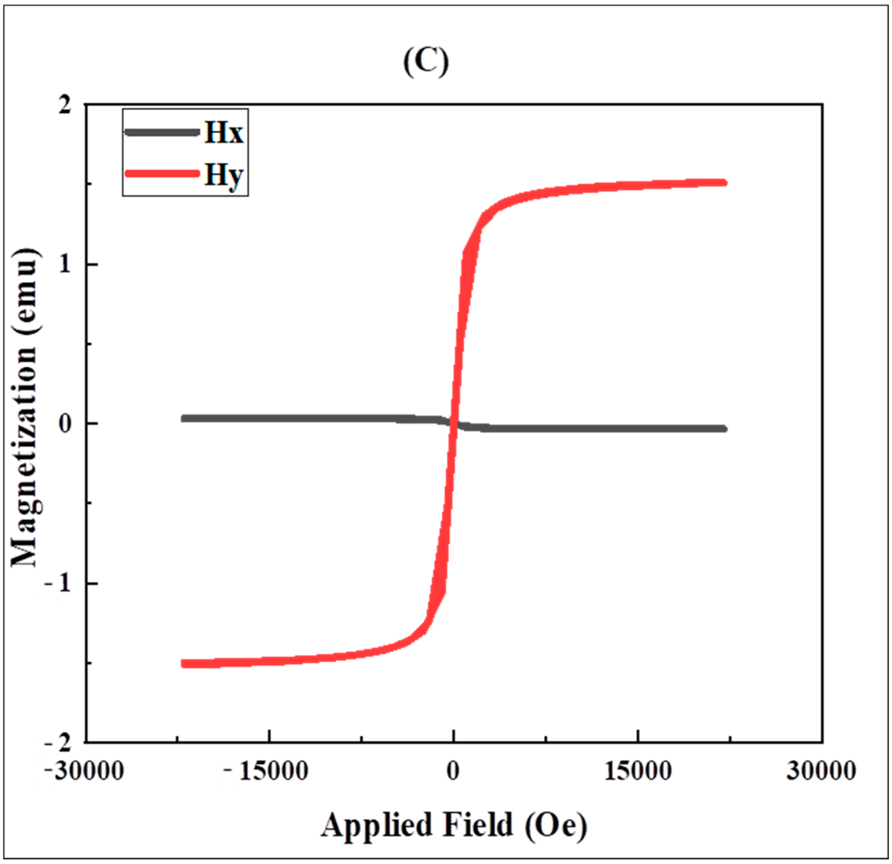

Figure 11. VSM for concentrate of (**A**) sample A, (**B**) sample B, and (**C**) sample C.

Moreover, sample C had a minimum magnetization of −1.51 emu, and as the percentage of iron decreased, so did the magnetization, as samples A and B showed magnetization of −0.76 emu and −1.15 emu. It is evident from these results that the percentage of iron influenced the magnetic properties, and the magnetic saturation tends to increase with the iron content.

3.4. Recovery and Grade Calculations

After magnetic separation, the concentrate and tailings were separated. Furthermore, moisture content was removed via filtration, followed by evaporation. The influence of magnetic separation on the grade and recovery of the concentrate was also evaluated by using Equations (4) and (5). Figure 12 presents the grade and recovery with respect to the drum wet weak magnetic separator's current. As the grade increased, recovery showed a decreasing trend.

Optimal results were obtained at 5 amperes, where the grade was recorded at 56%, and the recovery was about 75%. The results are in agreement with other findings reported by previous researchers [18,37]. As the current decreased, so did the magnetic intensity, and only highly magnetic particles such as free iron were seen in the concentrate, with a limited amount of magnetite. In addition, increasing the separator's current increased the magnetic intensity, and at the maximum current, coal was observed as a major impurity in the concentrate, reducing the overall grade.

3.5. Cost Estimation

Multiple factors play a vital role in cost estimations [38], and Figure 13 presents a selection of the factors. Local industries in Pakistan pay around USD 140-150 per dry metric ton for iron ore with >60% iron as compared to hematite ore (having 45% iron content) at USD 50 per dry metric ton and coal at USD 120 per dry metric ton (coal with a 20 weight percent hematite concentration costs USD 24), and local electricity charges are USD 0.15 per kWh consumption; thus, 6 h for a single process (3 h for size reduction and classification, 2 h for the reduction roasting process, and 1 h for magnetic separation) would cost around USD 45 per process, as the electricity consumed will be about 50 kW for a single process [39]. This reduction of ore from hematite to magnetite in the given conditions (at a laboratory scale) costs about USD 119 for the whole process, as compared to USD 150 when purchasing magnetite directly from an international supplier. This cost can be further reduced by several orders of magnitude if the same technique is carried out at a larger commercial scale.

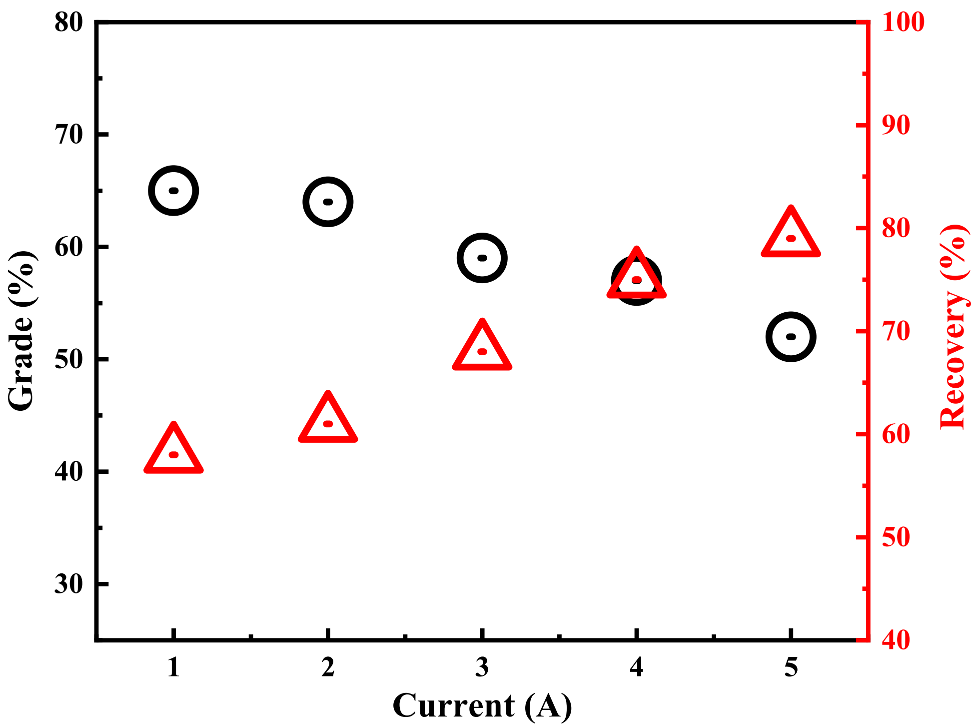

Figure 12. Current, grade, and recovery relationship of final beneficiated ore.

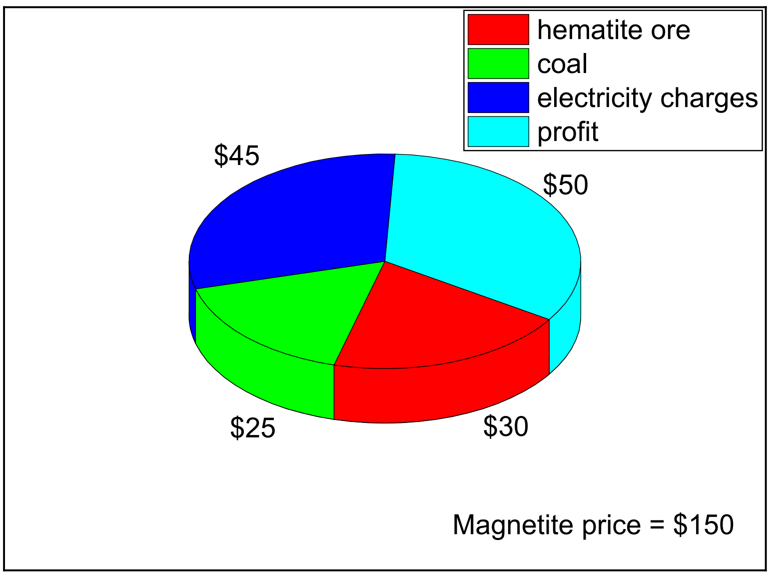

Figure 13. Cost distribution of magnetite in comparison to the whole process.

4. Conclusions

The reduction roasting of Dilband iron ore was carried out at high temperatures with the aim to enhance the Fe content in ore obtained from local Pakistani deposits. In addition, the magnetic properties of the ore were also determined using VSM. The results suggest that excellent reduction can be achieved at 900 °C for 2 h with a coal/ore ratio of 20 wt. %. The iron content/Fe concentration was increased from 34 to 56 wt. %. The yield, which was discovered to be around 75% weight percent, was also very high. Additionally, after roasting, strong magnetic behavior was induced, i.e., 1.5 emu. Furthermore, the enrichment of Dilband iron also provides an economically feasible product as compared to high-quality iron ore, which makes reduction roasting a potential process for the enrichment of the ore. The encouraging results clearly suggest that locally available Dilband ore has a huge potential to be used by the iron and steel sector operating in Pakistan. The estimated cost for the processing of Dilband ore is around 30% less than the cost of ore purchased from abroad. This also is a favorable factor that can be further reduced if the same process is carried out on a regular and larger scale.

Author Contributions: Conceptualization, A.D.C. and I.A.C.; methodology, A.A.S. (Asif Ahmed Shaikh), S.B.H.R., A.A.S. (Aqeel Ahmed ShahZ) and S.M.; writing, I.A.C., S.M., and J.A.; validation, I.A.C., A.D.C. and M.A.S.; investigation, J.A., I.A.C., and S.B.H.R.; supervision, A.D.C. and A.A.; funding acquisition, A.D.C. and A.A. All authors have read and agreed to the published version of the manuscript.

Funding: Research support from NED University of Engineering & Technology, Karachi, Pakistan.

Institutional Review Board Statement: Not applicable.

Informed Consent Statement: Not applicable.

Data Availability Statement: Data are available upon request from the corresponding authors.

Acknowledgments: The authors would like to acknowledge the Researcher's Supporting Project Number (RSP2023R269), King Saud University, Riyadh, Saudi Arabia, for their support in this work.

Conflicts of Interest: The authors declare no conflict of interest. The authors declare that they have no known competing financial interests or personal relationships that could have appeared to influence the work reported in this paper.

References

1. Roy, S.K.; Nayak, D.; Rath, S.S. A review on the enrichment of iron values of low-grade Iron ore resources using reduction roasting-magnetic separation. *Powder Technol.* **2020**, *367*, 796–808. [CrossRef]
2. He, J.; Liu, C.; Hong, P.; Yao, Y.; Luo, Z.; Zhao, L. Mineralogical characterization of the typical coarse iron ore particles and the potential to discharge waste gangue using a dry density-based gravity separation. *Powder Technol.* **2019**, *342*, 348–355. [CrossRef]
3. Khoso, S.A.; Lyu, F.; Meng, X.; Hu, Y.; Sun, W. Selective separation of chalcopyrite and pyrite with a novel and non-hazardous depressant reagent scheme. *Chem. Eng. Sci.* **2019**, *209*, 115204. [CrossRef]
4. Khoso, S.A.; Abro, M.I.; Agheem, M.H. Evaluation of Mesh of Liberation of Zard Koh and Kulli Koh Iron Ores of Pakistan. *Mehran Univ. Res. J. Eng. Technol.* **2018**, *37*, 569–580. [CrossRef]
5. Agrawal, A.; Das, K.; Singh, B.K.; Singh, R.S.; Tripathi, V.R.; Kundu, S.; Padmapal; Ramna, R.; Singh, M.K. Means to cope with the higher alumina burden in the blast furnace. *Ironmak. Steelmak.* **2020**, *47*, 238–245. [CrossRef]
6. Hanumanthappa, H.; Vardhan, H.; Mandela, G.R.; Kaza, M.; Sah, R.; Shanmugam, B.K. A comparative study on a newly designed ball mill and the conventional ball mill performance with respect to the particle size distribution and recirculating load at the discharge end. *Miner. Eng.* **2020**, *145*, 106091. [CrossRef]
7. Hanumanthappa, H.; Vardhan, H.; Mandela, G.R.; Kaza, M.; Sah, R.; Shanmugam, B.K.; Pandiri, S. Investigation on Iron Ore Grinding based on Particle Size Distribution and Liberation. *Trans. Indian Inst. Met.* **2020**, *73*, 1853–1866. [CrossRef]
8. Wasim, M.; Tariq, A.; Shafique, M.A.; Qureshi, R.N. Characterization and differentiation of iron ores using X-ray diffractometry, k_0 instrumental neutron acti-vation analysis and inductively coupled plasma optical emission spectrometry. *J. Radioanal. Nucl. Chem.* **2020**, *323*, 179–187. [CrossRef]
9. Yu, J.; Han, Y.; Li, Y.; Gao, P. Recent Advances in Magnetization Roasting of Refractory Iron Ores: A Technological Review in the Past Decade. *Miner. Process. Extr. Met. Rev.* **2020**, *41*, 349–359. [CrossRef]
10. Ponomar, V.P.; Brik, O.B.; Cherevko, Y.I.; Ovsienko, V.V. Kinetics of hematite to magnetite transformation by gaseous reduction at low concentration of coal mon-oxide. *Chem. Eng. Res. Des.* **2019**, *148*, 393–402. [CrossRef]

11. Roy, S.; Nayak, D.; Dash, N.; Dhawan, N.; Rath, S.S. Microwave-assisted reduction roasting—Magnetic separation studies of two mineralogically different low-grade iron ores. *Int. J. Miner. Met. Mater.* **2020**, *27*, 1449–1461. [CrossRef]
12. Chun, T.; Zhu, D.; Pan, J. Simultaneously Roasting and Magnetic Separation to Treat Low Grade Siderite and Hematite Ores. *Miner. Process. Extr. Met. Rev.* **2015**, *36*, 223–226. [CrossRef]
13. Quast, K. A review on the characterisation and processing of oolitic iron ores. *Miner. Eng.* **2018**, *126*, 89–100. [CrossRef]
14. Zhang, H.; Zhang, Z.; Luo, L.; Yu, H. Behavior of Fe and P during reduction magnetic roasting-separation of phosphorus-rich oolitic hematite. *Energy Sources Part A Recovery Util. Environ. Eff.* **2019**, *41*, 47–64. [CrossRef]
15. Dauce, P.D.; de Castro, G.B.; Lima, M.M.F.; Lima, R.M.F. Characterisation and magnetic concentration of an iron ore tailings. *J. Mater. Res. Technol.* **2019**, *8*, 1052–1059. [CrossRef]
16. Sahu, S.N.; Sharma, K.; Barma, S.D.; Pradhan, P.; Nayak, B.K.; Biswal, S.K. Utilization of low-grade BHQ iron ore by reduction roasting followed by magnetic separation for the pro-duction of magnetite-based pellet feed. *Metall. Res. Technol.* **2019**, *116*, 611. [CrossRef]
17. Ponomar, V.; Dudchenko, N.; Brik, A. Synthesis of magnetite powder from the mixture consisting of siderite and hematite iron ores. *Miner. Eng.* **2018**, *122*, 277–284. [CrossRef]
18. Yu, J.; Han, Y.; Li, Y.; Gao, P. Beneficiation of an iron ore fines by magnetization roasting and magnetic separation. *Int. J. Miner. Process.* **2017**, *168*, 102–108. [CrossRef]
19. Tang, Z.; Gao, P.; Li, Y.; Han, Y.; Li, W.; Butt, S.; Zhang, Y. Recovery of iron from hazardous tailings using fluidized roasting coupling technology. *Powder Technol.* **2020**, *361*, 591–599. [CrossRef]
20. Oritola, S.F.; Saleh, A.L.; Mohd Sam, A.R. Characterization of Iron Ore Tailings as Fine Aggregate. *ACI Mater. J.* **2020**, *117*, 125–134.
21. Valerevich Lvov, V.; Sergeevich Chitalov, L. Sergeevich Chitalov, and Technology, Comparison of the different ways of the ball Bond work index determining. *Int. J. Mech. Eng. Technol.* **2019**, *10*, 1180–1194.
22. Ahmad, S.; Channa, I.A. Mathematical Relationship between Ferritic, Pearlitic and Average Grain Size of Steel. *J. Mod. Sci. Technol.* **2013**, *1*, 1–18.
23. Peng, T.; Gao, X.; Li, Q.; Xu, L.; Luo, L.; Xu, L. Phase transformation during roasting process and magnetic beneficiation of oolitic-iron ores. *Vacuum* **2017**, *146*, 63–73. [CrossRef]
24. Ravisankar, V.; Venugopal, R.; Bhat, H. Investigation on beneficiation of goethite-rich iron ores using reduction roasting followed by magnetic separation. *Miner. Process. Extr. Metall. Trans. Inst. Min. Metall.* **2019**, *128*, 175–182. [CrossRef]
25. Pasechnik, L.; Skachkov, V.; Bogdanova, E.; Chufarov, A.Y.; Kellerman, D.; Medyankina, I.; Yatsenko, S. A promising process for transformation of hematite to magnetite with simultaneous dissolution of alumina from red mud in alkaline medium. *Hydrometallurgy* **2020**, *196*, 105438. [CrossRef]
26. Abro, S.H.; Chandio, A.; Siddiqui, M.A.; Channa, I.A. Aluminum and aluminum nitrides effect on nucleation sites in micro-alloyed steel. *Proc. Pak. Acad. Sci. Part B* **2019**, *56*, 17–26.
27. Maitlo, I.; Aftab, U.; Abro, M.I.; Baloch, M.M. Selective Leaching of Steel Pollutant Element from Dilband Iron Ore, Pakistan. *Mehran Univ. Res. J. Eng. Technol.* **2017**, *36*, 757–762. [CrossRef]
28. Makhdoom, M.A.; Ahmed, F.; Channa, I.A.; Inam, A.; Riaz, F.; Siyal, S.H.; Shar, M.A.; Alhazaa, A. Effect of Multiple Thermal Cycles on the Microstructure and Mechanical Properties of AISI 1045 Weldments. *ACS Omega* **2022**, *7*, 42313–42319. [CrossRef]
29. Ezhov, A.; Shvaljov, Y. Dry Magnetic Separation of Iron Ore of the Bakchar Deposit. *Procedia Chem.* **2015**, *15*, 160–166. [CrossRef]
30. Xiao, J.; Zhou, L. Increasing Iron and Reducing Phosphorus Grades of Magnetic-Roasted High-Phosphorus Oolitic Iron Ore by Low-Intensity Magnetic Separation–Reverse Flotation. *Processes* **2019**, *7*, 388. [CrossRef]
31. Dash, N.; Rath, S.S.; Angadi, S.I. Thermally assisted magnetic separation and characterization studies of a low-grade hematite ore. *Powder Technol.* **2019**, *346*, 70–77. [CrossRef]
32. Harano, T.; Nemoto, Y.; Murao, R.; Kimura, M. Accuracy Improvement of the XRD-Rietveld Method for the Quantification of Crystalline Phases in Iron Sintered Ores through the Correction of Micro-absorption Effects. *ISIJ Int.* **2020**, *60*, 2851–2858. [CrossRef]
33. Ardiani, N.R.; Setianto, S.; Santosa, B.; Wibawa, B.M.; Panatarani, C.; Joni, I.M. Quantitative analysis of iron sand mineral content from the south coast of Cidaun, West Java using rietveld refinement method. In Proceedings of the AIP Conference Proceedings 2nd International Conference and Exhibition on Powder Technology (ICePTi), Solo, Indonesia, 20–21 August 2019; AIP Publishing LLC: Bandung, Indonesia. [CrossRef]
34. Zhu, X.; Han, Y.; Sun, Y.; Li, Y.; Wang, H. Siderite as a novel reductant for clean utilization of refractory iron ore. *J. Clean. Prod.* **2020**, *245*, 118704. [CrossRef]
35. Gao, L.; Liu, Z.; Pan, Y.; Ge, Y.; Feng, C.; Chu, M.; Tang, J. Separation and Recovery of Iron and Nickel from Low-Grade Laterite Nickel Ore Using Reduction Roasting at Rotary Kiln Followed by Magnetic Separation Technique. *Min. Metall. Explor.* **2018**, *36*, 375–384. [CrossRef]
36. Campos, T.M.; Bueno, G.; Rodriguez, V.A.; Boettcher, A.C.; Kwade, A.; Mayerhofer, F.; Tavares, L.M. Relationships between particle breakage characteristics and comminution response of fine iron ore con-centrates. *Miner. Eng.* **2021**, *164*, 106818. [CrossRef]
37. Zhang, X.; Han, Y.; Sun, Y.; Lv, Y.; Li, Y.; Tang, Z. An Novel Method for Iron Recovery from Iron Ore Tailings with Pre-Concentration Followed by Magnetization Roasting and Magnetic Separation. *Miner. Process. Extr. Met. Rev.* **2020**, *41*, 117–129. [CrossRef]

38. Purohit, S.; Ekman, B.; Mejias, R.; Brooks, G.; Rhamdhani, M.A. Solar processing of composite iron ore pellets: Preliminary assessments. *J. Clean. Prod.* **2018**, *205*, 1017–1028. [CrossRef]
39. Palacios, J.-L.; Fernandes, I.; Abadias, A.; Valero, A.; Valero, A.; Reuter, M.A. Avoided energy cost of producing minerals: The case of iron ore. *Energy Rep.* **2019**, *5*, 364–374. [CrossRef]